Thermochimica Acta, 231 (1994) 203–213
Elsevier Science B.V., Amsterdam
SSDI 0040-6031(93)01342-Z

Polymer melting: heating rate effects on DSC melting peaks

Ge Wang and Ian R. Harrison *

Polymer Science Program, Department of Materials Science and Engineering,
The Pennsylvania State University, University Park, PA 16802 (USA)

(Received 30 March 1993; accepted 17 April 1993)

Abstract

The effect of heating rate on DSC peak shape has been investigated using Gray's model. Theoretical DSC melting curves for small samples with sharp transition temperatures were created and compared with DSC melting curves from pure indium samples. Good agreement was found between theoretical curves and experimental indium DSC peaks. As heating rate increases, there is an increase in both peak height and the time necessary for the sample to catch up with the programmed temperature. For pure indium samples the slope of the leading edge of the first half-peak shows no variation with increase in heating rate when plotted versus temperature. With increasing heating rate the melting peak appears narrower when heat flow is plotted versus time, and broader when plotted against temperature. Peak height dependence on heating rate was found to be somewhat more noticeable at lower heating rates than at higher rates. However, samples formed from a mixture of polyethylene (PE) and indium powder had melting curves that are quite different from those of pure indium. Significant variation in the slope of the first half-peak with heating rate results from changes in thermal resistance from sample surface to the interior. This information helps develop our understanding of, and aids in interpreting, ordinary DSC results.

INTRODUCTION

Differential scanning calorimetry (DSC) is a powerful tool widely used in material characterization. Transition temperatures and other important information can be derived from peak analysis. For example, DSC has been used to determine crystallinity [1,2], heat capacity [3–5], purity [6–8], and crystallization and reaction kinetic parameters [9–11]. Even approximations of lamellae thickness distributions have reportedly been derived from analysis of melting peaks [12]. Thermal properties of a polymer are closely

---

* Corresponding author.

0040-6031/94/$07.00 © 1994 – Elsevier Science B.V. All rights reserved

related to molecular and morphological structures, and therefore mechanical behavior. As a result of its broad applicability the importance of DSC analysis in material research cannot be overstated.

The usefulness of this technique, however, is often limited by difficulties in understanding and interpreting experimental results. Many factors, such as size, packing, form (powder, film, particles), pan contact and position, purging gas and its flow rate, and experimental heating rate all affect DSC thermal curves and therefore compound data interpretation problems.

In this paper, the effect of heating rate on the melting peak is discussed based largely on Gray's original formulation [13]. Experimental DSC curves obtained using indium powder samples are compared with theoretical curves. Overall features such as peak width, height, initial slope, time to melt, and time for the sample to catch up with the programmed temperature were all examined. This work was extended to include heating rate effects in idealized polymer samples modeled with polymer/indium powder mixtures.

EXPERIMENTAL

Indium powder (size, 150 mesh; purity, 99.99%) was used for pure indium samples, and to prepare a polymer/indium mixture with high density polyethylene (HDPE). To mix indium powder and HDPE, the powder was evenly spread on HDPE blown film and then covered by another HDPE film. This sandwich was placed between Teflon coated aluminum sheets and pressed at 150°C. After pressing, the newly formed PE/indium powder film was folded once in half and repressed. This latter process was repeated about 25 times. The final film was visually inspected to ensure uniform distribution of indium within the PE matrix. In this way approximately 5% by weight of indium was incorporated in HDPE film. To make sure that the sample is in good contact with the sample pan, a paper hole punch was used to cut the PE/indium film into circular pieces which exactly fit aluminum DSC pans. The sample pan bottom was flattened after sealing.

All DSC tests were performed on a Perkin–Elmer DSC 7 instrument and data transferred from the Perkin-Elmer computer into ASCII format. A computer program was written in c language to analyze experimental DSC data and to create computer simulated DSC curves.

THEORETICAL DSC PEAK ANALYSIS

For very small samples a model for melting peak shape has been developed by Gray based on energy conservation and Newton's law. The melting peak shape for such a small sample has been shown to consist of two half-peaks, the first half-peak has a straight line slope and the second

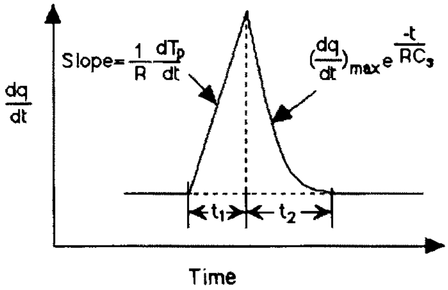

Fig. 1. Schematic representation of a sharp transition DSC peak.

half-peak shows an exponentially decaying curve (see Fig. 1). Equations describing the two half-peaks are for the first half-peak

$$\frac{\mathrm{d}q}{\mathrm{d}t}=\frac{1}{R}\frac{\mathrm{d}T_\mathrm{p}}{\mathrm{d}t}t \tag{1}$$

and for the second half-peak

$$\frac{\mathrm{d}q}{\mathrm{d}t}=\left(\frac{\mathrm{d}q}{\mathrm{d}t}\right)_\mathrm{max}\exp\left(\frac{-t}{RC_\mathrm{s}}\right) \tag{2}$$

where $\mathrm{d}q/\mathrm{d}t$ is heat flow rate, R is thermal resistance, C_s is the total sample heat capacity, $\mathrm{d}T_\mathrm{p}/\mathrm{d}t$ is heating rate, and t is time.

From eqns. (1) and (2), we see that heating rate affects the slope of the first half-peak. As heating rate increases, the slope becomes steeper and the whole melting peak becomes narrower. In order to understand the effects of heating rate on overall melting peak shape, we need to determine parameters such as peak height $(\mathrm{d}q/\mathrm{d}t)_\mathrm{max}$, the time needed for the crystalline material in the sample to melt (t_1) and the time needed for the sample temperature to catch up with programmed temperature (t_2). Theoretically t_2 will be infinitely long; however, for practical purposes, t_2 can be defined as the time for $\mathrm{d}q/\mathrm{d}t$ to fall below 1% of its maximum value. Regardless of how peak shape changes, the total energy required to melt the same amount of material remains constant, i.e. peak area is a constant. With this in mind, we can determine how heating rate affects t_1 and t_2.

The total energy to melt the material (ΔH) can be obtained by integration from the onset to the end of melting, i.e. from $t=0$ to $t=t_1$

$$\Delta H=\int\frac{\mathrm{d}q}{\mathrm{d}t}\mathrm{d}t=\frac{\mathrm{d}T_\mathrm{p}}{\mathrm{d}t}\frac{t_1^2}{2R}+C_\mathrm{s}\frac{\mathrm{d}T_\mathrm{p}}{\mathrm{d}t}t_1 \tag{3}$$

Solving this equation, we find

$$t_1=RC_\mathrm{s}\left[\sqrt{1+\frac{2\Delta \mathrm{H}}{RC_\mathrm{s}^2\frac{\mathrm{d}T_\mathrm{p}}{\mathrm{d}t}-1}}\right] \tag{4}$$

Rearranging eq. (2) gives

$$t_2 = RC_s \ln\left[\frac{\left(\frac{\mathrm{d}q}{\mathrm{d}t}\right)_{\max}}{\Delta}\right] = RC_s \ln(100) \tag{5}$$

where Δ represents the value $\mathrm{d}q/\mathrm{d}t$ where the peak tail can be considered essentially returned to baseline; in this case Δ is 1% of the difference between $(\mathrm{d}q/\mathrm{d}t)_{\max}$ and the baseline value.

Peak height from the baseline can be calculated by replacing t in eqn. (1) with t_1 from eq. (4); then

$$\left(\frac{\mathrm{d}q}{\mathrm{d}t}\right)_{\max} = \frac{\mathrm{d}T_{\mathrm{p}}}{\mathrm{d}t} C_s \left[\sqrt{1 + \frac{2\Delta H}{RC_s^2 \frac{\mathrm{d}T_{\mathrm{p}}}{\mathrm{d}t} - 1}}\right] \tag{6}$$

RESULTS AND DISCUSSION

Figure 2 shows four computer simulated DSC melting curves plotted as heat flow versus time for different heating rates. Since the equations are derived assuming identical thermal resistance within the whole sample, these curves are representative of melting behavior for very small samples with a sharp melting transition, e.g. indium. Differences between curves due to differences in heating rate are clearly displayed. At lower heating rates, the slope of the leading edge of the melting peak is small, as is peak height. The time t_1 needed to melt the sample at lower heating rates is considerably longer than that at higher heating rates. Because the peak height $(\mathrm{d}q/\mathrm{d}t)_{\max}$ for higher heating rates is greater than that for the lower heating rates, the time taken to return to baseline (t_2) is somewhat longer at higher heating rates than slower heating rates. Clearly, peak shape is very sensitive to changes in heating rate.

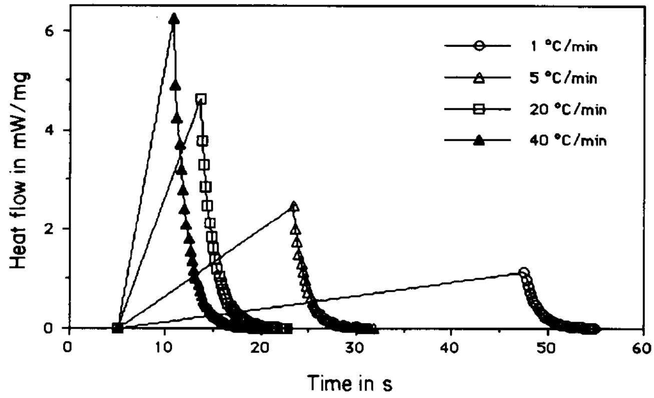

Fig. 2. Computer generated DSC curves for different heating rates: Heat flow vs. time; other parameters: $C_s = 15.0$ mJ °C^{-1}, $\Delta H = 230.0$ mJ, $R = 0.07$°C mW^{-1}.

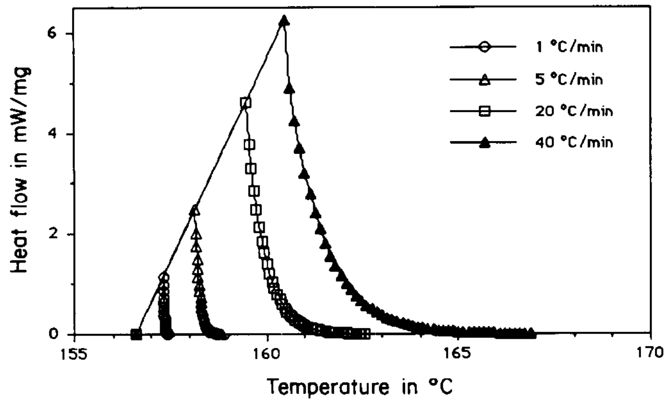

Fig. 3. DSC curves plotted as heat flow vs. temperature data from Fig. 2.

More usually DSC curves are plotted as heat flow versus programmed temperature (Fig. 3). In this case, the overall peak shapes will be different from the ones previously shown although the same data is used for Figs. 2 and 3. In particular, the peak area for different heating rates is no longer the same. Commercial software corrects for these area changes with heating rate when computing the heat of fusion of a sample. In addition, increasing heating rate results in a broader peak, when plotted versus temperature, as opposed to a narrowing of the peak when plotted versus time, as shown in Fig. 2. Finally, the slope of the melting peak is not affected by heating rate. When the curve is plotted as heat flow against temperature, the time axis is multiplied by the heating rate, and the slope becomes a constant with a value of $1/R$.

To test the validity of the model, a small, high purity indium sample was run in the DSC. Melting curves obtained at different heating rates are shown in Fig. 4. The instrument needs to be calibrated at each heating rate to ensure that the onset of melting occurs at the same temperature in all cases. Comparing these experimental curves with the computer created ones shown in Figs. 2 and 3, we see essentially the same heating rate effects on the melting peak. When data is plotted as heat flow versus time, as heating rate increases (Fig. 4(a)), the peak height and the slope of the peak leading edge increases, while the time needed to melt the sample decreases. When plotted as heat flow versus temperature (Fig. 4(b)), the peak broadens as the heating rate increases while the leading edge slope remains constant.

Another interesting feature observed in both theoretical and experimental DSC curves is that the peak height height increases dramatically with heating rate at the lower heating rates; at higher heating rates, differences between peak heights become somewhat smaller. Figure 5 shows a plot of peak height versus heating rate calculated using eqn. (6) and the

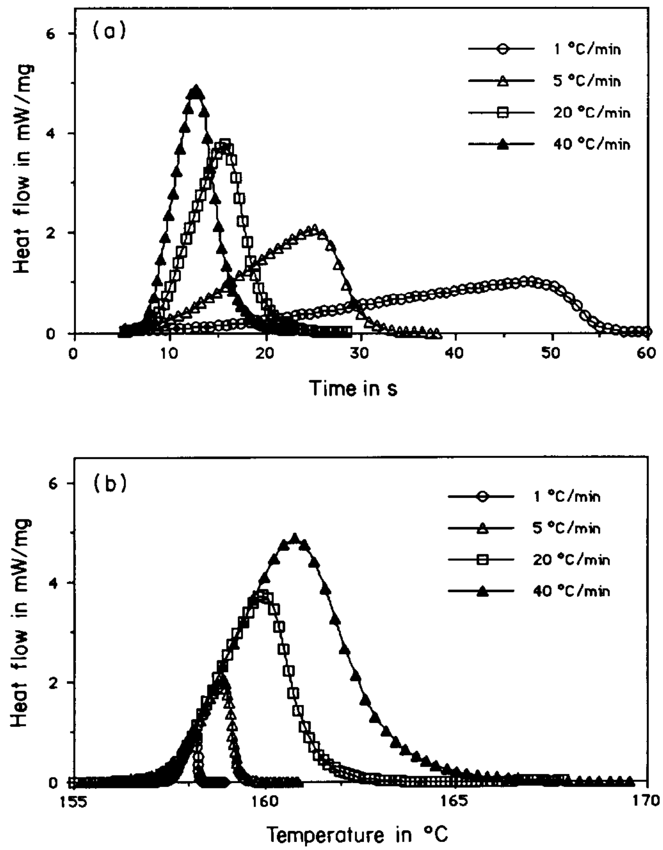

Fig. 4. Heating rate effects on a pure indium sample; (a) DSC curves plotted as heat flow vs. time; (b) DSC curves plotted as heat flow vs. temperature.

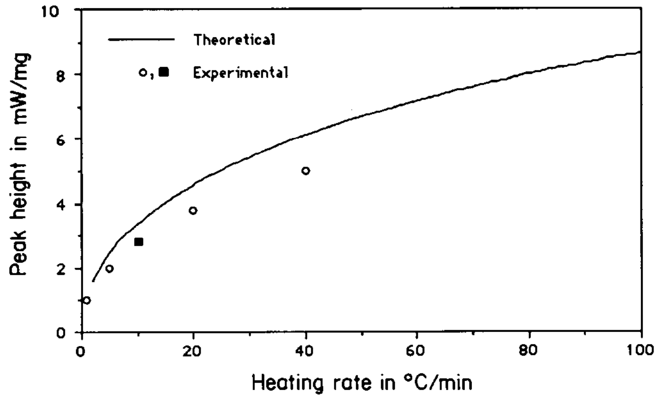

Fig. 5. Theoretical peak height vs. heating rate; model parameters as used for Fig. 2. Experimental peak heights from Fig. 4(b), ○ and a 10°C min^{-1} sample (■) are also shown.

parameters used for creating DSC curves shown in Fig. 2. In this particular case, the greatest increase in peak height occurrs at heating rates below about 10°C Min^{-1}; peak height changes becomes less pronounced as heating rate increases.

This indium heating rate study was to serve as a basis for understanding how polymer systems respond under different heating rates. We know that a semicrystalline polymer's melting behavior is quite different from that of indium because of the polymer's partial crystallinity, low thermal conductivity and density. For the same weight of sample, polymer would be significantly larger than indium and therefore have more pronounced size effects. Conductivity and density differences between indium and polymer result in considerable differences in thermal resistance within the sample. Our previous investigations have shown that for a 0.32 mm thick polyethylene sample (about 10 mg), thermal resistance at the bottom of the sample is only half that in the middle [14]. Naturally, for thicker samples, thermal resistance differences are even greater. We therefore anticipate that heating rate effects in polymer melting cannot be accurately described by a Gray type model which uses fixed R values.

In order to more easily examine and interpret rate effects in polymer melting transitions, we need a polymer sample with a single sharp melting transition which is uncomplicated by annealing or other reorganizational phenomena. The sample should model a semicrystalline polymer with sharply melting crystals randomly dispersed in an amorphous matrix. The low thermal conductivity feature of such a sample should not change significantly during melting and therefore allow close simulation of an idealized polymer melting process. A sample made of PE/indium powder with about 5% by weight of indium was prepared to meet these requirements.

Figure 6 shows four DSC curves of the indium portion of the transition

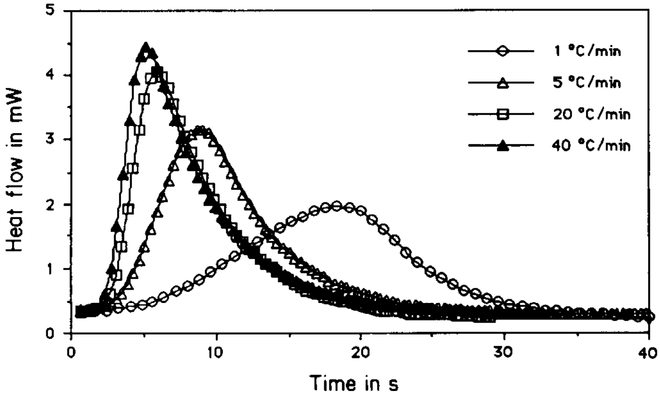

Fig. 6. DSC curves plotted as heat flow vs. time for samples of PE/indium powder mixture tested at different heating rates.

plotted as heat flow versus time for PE/indium samples tested at different heating rates. In this and subsequent plots indium powder is melting in an already molten PE matrix. In addition, curves are shifted along the time axis so that the onset of melting is superimposed. General heating rate effects on the melting peak appear similar to those observed for pure indium. As heating rate increases the melting peak increases in height, and the slope of the leading edge of the first half peak also increases.

However, when these PE/indium powder samples are plotted as heat flow versus temperature (Fig. 7), we see quite distinct differences when compared to pure indium samples (Fig. 4(b)). For pure indium samples the ratio of t_1 to t_2 is such that the peak maximum is skewed to the high temperature side of the peak at all heating rates examined. With PE/indium powder the reverse is true and, as heating rate increases, t_2

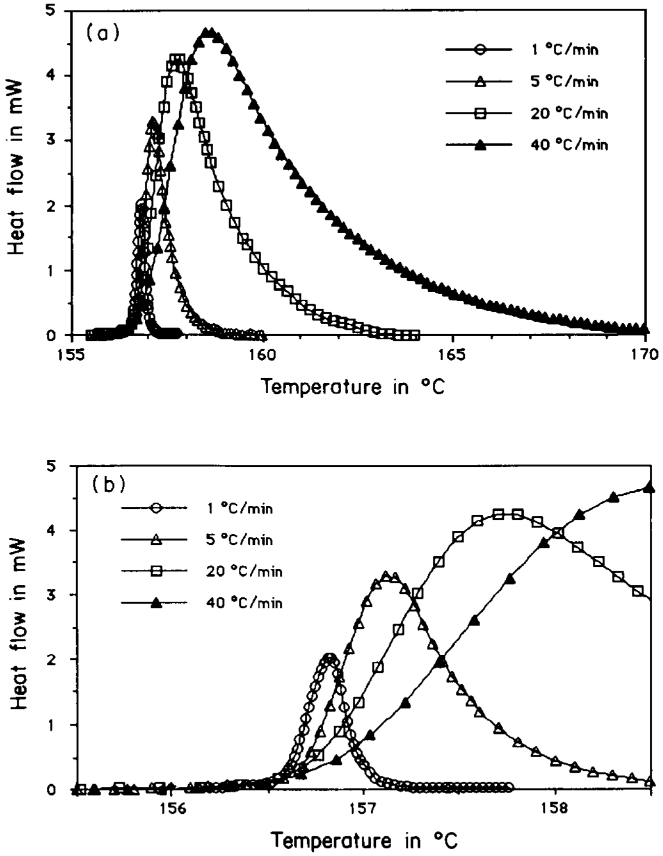

Fig. 7. DSC data shown in Fig. 6 plotted as heat flow vs. temperature: (a) overall melting peak; (b) expanded first half melting peak. Curves at different heating rates are shifted to give the same onset temperature as pure indium.

increases dramatically. This is mainly attributable to thermal resistance and sample size differences previously described.

For the pure indium sample, its high thermal conductivity allows rapid heat flow into the sample. Any thermal resistance increase due to molten indium is negligible and the sample essentially has a constant *R* throughout; there is no variation in the slope of the peak as heating rate changes. However, for PE/indium powder samples, a significant variation in thermal resistance exists for different positions within the sample. Such variation results from the low thermal conductivity of the polymer matrix. Considering the large differences in thermal conductivity between the surrounding aluminum pan and the polymer matrix, it is reasonable to envision that melting first occurs in a thin outer shell of the PE/indium sample. Melting then progresses shell after shell from the outside shell to the middle of the sample (Fig. 8).

As melting proceeds, thermal resistance increases for the next shell due to contributions from the previously melted shell, i.e. the effective *R* increases as the melt front moves from the sample outside to its interior. This thermal resistance difference between sample surface and its interior causes the largest sample volume, i.e. the outside shell, to melt faster and the smaller interior shell to melt slower. The overall melting curve is the summation of all shell contributions; thus, the peak maximum skews toward the low temperature side of the peak. This does not mean that the overall melting curve for a PE/indium powder sample necessarily has a lower temperature maximum than pure indium. For a comparable weight of indium the pure indium sample generally has a lower maximum temperature; however the PE/indium mixture has its peak maximum skewed to the low temperature side of its overall melting peak. As an example Fig. 9 shows a comparison between pure indium and PE/indium powder both run at 20°C min^{-1}. Note that the onset of melting for the PE/indium sample is also shifted to a somewhat higher temperature compared to that for pure indium. This shift presumably results from the thermal resistance of surface

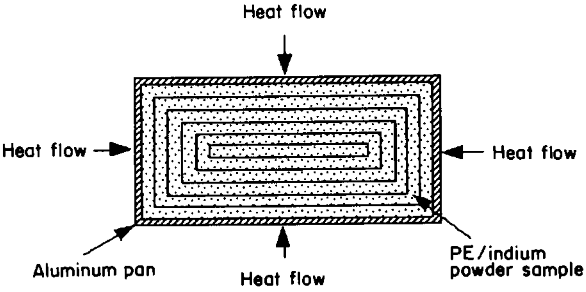

Fig. 8. Schematic illustration of PE/indium sample melting process.

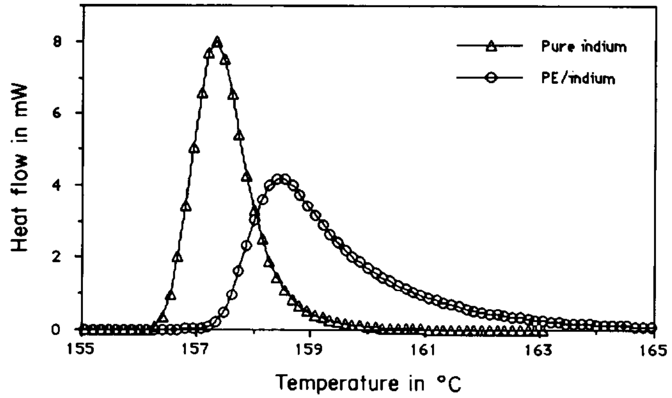

Fig. 9. Comparison between DSC curves from pure indium and a PE/indium sample containing a comparable amount of indium (about 1 mg) run at 20°C $\min^{-1}$.

layers which are rich in PE (compared to pure indium) and delay the onset of melting.

Another major difference between pure indium and PE/indium is seen in the slope of the first half-peak. Unlike pure indium the PE/indium sample does not show a constant slope for the first half-peak for all heating rates. For PE/indium samples, at lower heating rates, e.g. 1°C $\min^{-1}$ and 5°C $\min^{-1}$, the slope of the first half peak appears to be largely unaffected by heating rate. However, at higher heating rates, the slope is reduced as heating rate increases. This is more clearly seen in Fig. 7(b) which is an expansion of the first half-peaks for the same curves shown in Fig. 7(a). The decrease in slope suggests that R changes at higher heating rates. This can be rationalized based on Newton's law ($\mathrm{d}q/\mathrm{d}t = \Delta T/R$). At very low heating rates, there is enough time ($\mathrm{d}t$) for the required small amount of heat ($\mathrm{d}q$) to flow into the sample to eliminate the small temperature difference between programmed temperature and sample temperature (ΔT). At higher heating rates, ΔT is larger and greater heat flow ($\mathrm{d}q/\mathrm{d}t$) is needed to eliminate it. If this required heat flow cannot be effectively introduced into the sample, this is equivalent to saying that the sample has a greater R value. The difficulty in transferring heat in these PE/indium samples versus pure indium arises from the lower thermal conductivity of the PE matrix.

SUMMARY AND CONCLUSIONS

Theoretical DSC melting curves for small samples with sharp transition peaks were created based on Gray's approach, and pure indium powder was run in a DSC with different heating rates. Good agreement was found between theoretical curves and experimental indium DSC curves. As heating rate increases, peak height, and time for the sample to catch up with programmed temperature both increase. The thermal resistance for pure indium samples shows no significant variation with heating rate. With increasing heating rate the melting peak appears narrower when heat flow is plotted versus time, and broader when plotted against temperature. Peak height dependence with heating rate was found to be somewhat more noticeable at lower heating rates than at higher rates.

PE/indium powder samples were also examined using DSC. This sample simulates a polymer system in which mono distributed single melting point lamellae, which are incapable of "reorganizing", are uniformly distributed in an amorphous matrix. As a function of heating rate PE/indium powder samples exhibit quite different melting behavior from that of pure indium. Thermal resistance differences within the PE/indium sample manifest themselves as variations in the slope of the leading edge of the peak.

This study systematically explores the effect of heating rate on peak height, width and shape. This information is helpful in understanding and interpreting ordinary DSC data; it is also extremely useful in understanding how thermal resistance and heating rate affect practical melting processes. Further adaptations of Gray's model are being pursued to fully describe the real melting process of polymer systems.

ACKNOWLEDGMENTS

The authors thank SAIC(13-910014-43) and NASA (Wallops Ballons) for partial support of this work.

REFERENCES

1 N.T. Wakdyn and P.R. Young, J. Appl. Polymer. Sci., 10 (1966) 1421.
2 M.J. Dole, J. Polym. Sci., Polym. Symp., 18 (1967) 57.
3 M.J. O'Neill, Anal. Chem., 38 (1966) 1331.
4 A.P. Gray, Polym. Prepr. Am. Chem. Soc. Div. Polym. Chem., 6(2) (1966) 956.
5 Thermal Analysis Newsletter No. 3, Perkin-Elmer Corporation, Norwalk, CT.
6 G.L. Driscoll, I.N. Duling, F. Magnotta, in R.S. Porter and J.F. Johnson (Eds.), Proc. Am. Chem. Soc. Symp. Analytical Calorimetry, San Francisco, CA, April 2–5, 1968, p. 271.
7 Thermal Analysis Newsletter No. 5, Perkin-Elmer Corporation, Norwalk, CT.
8 C. Plato and A.R. Glasgow, Jr., Anal. Chem., 41 (1969) 330.
9 J. Boon and J.M. Azcue, J. Polym. Sci. Polym. Phys. Ed., 6 (1968) 885.
10 J. Boon, G. Challa and D.W. Van Krevelen, J. Polym. Sci. Polym. Phys. Ed., 6 (1968) 1791.
11 P. Peyer and W.D. Bascom, in R.S. Porter and J.F. Johnson (Eds.), Proc. Am. Chem. Soc. Symp. Analytical Calorimetry, Los Angeles, CA, March 30–April 5, 1974, p. 537.
12 A. Wlochowicz and M. Eder, Polymer, 25 (1984) 1268.
13 A.P. Gray, in R.S. Porter and J.F. Johnson (Eds.), Proc. Am. Chem. Soc. Symp. Analytical Calorimetry, San Francisco, CA, April 2–5, 1968, p. 209.
14 G. Wang and I.R. Harrison, Thermochimica Acta, 230 (1993) 309.